ON THE APPLICATION OF ADAPTIVE GRIDS IN SOME MESOSCALE MODELS FOR NUMERICAL WEATHER PREDICTION

C. I. Christov
E. Rodriguez
J.-A. García-Moya
R. Díaz-Pabón

Servicio de Predicción Numerica, Instituto Nacional de Meteorologia,
C/de las Moreras s/n, Ciudad Universitaria, 28040 Madrid, ESPAÑA

ABSTRACT

In the present paper, the application of adaptive curvilinear coordinates in a 2D barotropic model for numerical weather prediction is considered. The necessary formulas for coordinate transformation are compiled and the governing equations of the model are recast in terms of generally non-orthogonal time-dependent curvilinear coordinates. An algorithm for elliptic mesh generation developed in earlier works of the authors is employed. Two different modes of application of adaptive meshes are outlined. In the first one, the curvilinear coordinates are condensed so as to improve the resolution over an a-priori defined subregion of the flow. In the second mode, the coordinates evolve in time as a result of the Jacobian being tuned to the gradients of the flow.

1. Introduction

The accuracy of numerical weather prediction depends very much on the computational mesh. Unfortunately, the mesh could not be refined to the utmost, because of the computational limitations. Then the problem arises of how to make the meshes finer in the sub-regions of special interest being coarse in the rest of computational domain. This can be done either through introducing additional grid points in the frame of cartesian coordinate system or by using special curvilinear coordinates that are either a-priori or being a-posteriori adapted to the flow. The first approach is called multigrid technique [1], [2], [3]. Its main advantage is concluded in the fact that the original coordinate system is used. The computations and reducing the accuracy of the difference formulas at the interfaces between the grid patches of different resolution. The second approach is called adaptive grids [1]. It has been extensively used in last two decades (see [4],[5],[6]) in Computational Fluid Mechanics (CFD). The disadvantage of this method is in the increased number of arithmetic operations per unit node which is the result of the introduction of non-uniform coefficients in the equations. The main advantages show up through flexibility of the grid and through the convenience in algoritmization, the latter due to the fact that the transformed region can always be made rectilinear. We consider in the present work the application of the method of adaptive grids.

Adaptive grids can be employed in numerical weather prediction in two main modes. In the first mode, a fixed non-uniform grid is introduced prior to

computations in order to improve the resolution over a specific area of the flow. Thus on can have magnitudes of spacings as small as for a fine grid while the boundary conditions (inlet and outlet conditions) are imposed as far off as in the coarse-grid large-scale models. In the second mode the adaptive grid evolves in time with the flow. There exists a number of different ways to establish correspondence between the mesh and the flow, but in fact, all of them aim at minimizing the truncation error or certain functional of it (see [4], [5], [6], [7] for general review and [1], [8], [9] - for review of applications to numerical weather prediction). In the present paper we follow the idea of [10] to keep the Jacobian of the coordinate transformation approximately proportional to the norm of the gradients of the flow and make use of the algorithms developed in [10], [11] and [12]. Results are presented for both fixed and moving adaptive grids.

2. The Barotropic Model

In order to elucidate the main problems related to application of adaptive grids in numerical weather prediction, it is convenient not to complicate much the very model. For this reason we consider here the barotropic 2D model on the sphere (see, e.g., [13]) for which the momentum equation then takes the form

$$\left(\frac{a\pi}{180}\right)^2 \cos\varphi \frac{\partial}{\partial t}\nabla^2\psi - \left[\frac{\partial\psi}{\partial y}\frac{\partial\nabla^2\psi}{\partial x} - \frac{\partial\psi}{\partial x}\frac{\partial\nabla^2\psi}{\partial y}\right] + 2\Omega\frac{\partial\sin\varphi}{\partial y}\frac{\partial\psi}{\partial x} = 0, \qquad (1)$$

$$\nabla^2 \equiv \left(\frac{180}{\pi}\right)^2\left[\frac{\partial^2}{\partial y^2} - \tan\varphi\frac{\partial}{\partial y} + \cos^{-2}\varphi\frac{\partial^2}{\partial x^2}\right], \quad \varphi \equiv \frac{\pi y}{180}, \qquad (2)$$

where y and x are, respectively the latitude and the longitude measured in degrees. The components of velocity are connected to the stream function through the standard relations

$$U = -\frac{180}{a\pi}\frac{\partial\psi}{\partial y}, \qquad V = \frac{180}{a\pi}\cos^{-1}\frac{\pi y}{180}\frac{\partial\psi}{\partial x} \qquad (3)$$

Introducing the so called total vorticity we render the momentum equation into the form

$$\left(a^2\cos\frac{\pi y}{180}\right)\frac{\partial\zeta}{\partial t} + \frac{D(\psi,\zeta)}{D(x,y)} = 0, \quad \zeta \equiv \nabla^2\psi + 2\Omega\sin\frac{\pi y}{180} \qquad (4)$$

In order not to abuse the size of present paper we do not cite here the exact form of the finite differences employed in the implementation of the barotropic model outlined. It suffices only to mention that we follow the implementation of [14], [15] with the necessary changes necessitated by the coordinate transformation. The main features of the implementation are the so-called Arakawa differencing (see [13] page 191, [16]) and iterational implicit convergence scheme for the equation for stream function.

3. Coordinate transformation

Consider the following general coordinate transformation

$$x = x(\xi,\eta;t)\,, \quad y = y(\xi,\eta;t)\ . \tag{5}$$

The sought functions ψ and ζ are compound functions of the curvilinear coordinates ξ and η, namely

$$\zeta(\xi,\eta;t) \equiv \zeta[x(\xi,\eta;t),y(\xi,\eta;t);t]\ . \tag{6}$$

Then for the first spatial derivatives we have

$$\zeta_x = \frac{y_\eta}{J}\zeta_\xi - \frac{y_\xi}{J}\zeta_\eta\,, \quad \zeta_y = \frac{x_\xi}{J}\zeta_\eta - \frac{x_\eta}{J}\zeta_\xi\,, \quad J \equiv \frac{D(x,y)}{D(\xi,\eta)}\ . \tag{7}$$

Here J is called Jacobian of the coordinate transformation. Respectively, the time derivative in terms of the new coordinates reads

$$\zeta_t = \zeta_t + \frac{-x_t y_\eta + y_t x_\eta}{J}\zeta_\xi + \frac{x_t y_\xi - y_t x_\xi}{J}\zeta_\eta\ . \tag{8}$$

Being reminded that the same formulas are valid for the spatial derivatives of ψ one rewrites the momentum equation as follows

$$a^2\cos\frac{\pi y}{180}\left[\frac{\partial\zeta}{\partial t} + \frac{x_t}{J}\frac{D(y,\zeta)}{D(\xi,\eta)} - \frac{y_t}{J}\frac{D(x,\zeta)}{D(\xi,\eta)}\right] + \frac{1}{J}\frac{D(\psi,\zeta)}{D(\xi,\eta)} = 0 \tag{9}$$

Respectively, for the second derivatives of the stream functions with respect to the curvilinear coordinates we have

$$\frac{\partial^2\psi}{\partial x^2} = \frac{y_\eta}{J}\frac{\partial}{\partial\xi}\left(\frac{y_\eta}{J}\psi_\xi - \frac{y_\xi}{J}\psi_\eta\right) - \frac{y_\xi}{J}\frac{\partial}{\partial\eta}\left(\frac{y_\eta}{J}\psi_\xi - \frac{y_\xi}{J}\psi_\eta\right)\,, \tag{10}$$

$$\frac{\partial^2\psi}{\partial y^2} = \frac{x_\eta}{J}\frac{\partial}{\partial\xi}\left(\frac{x_\eta}{J}\psi_\xi - \frac{x_\xi}{J}\psi_\eta\right) - \frac{x_\xi}{J}\frac{\partial}{\partial\eta}\left(\frac{x_\eta}{J}\psi_\xi - \frac{x_\xi}{J}\psi_\eta\right)\ . \tag{11}$$

Then the Laplace operator adopts the form

$$\frac{\partial^2\psi}{\partial x^2} + \frac{\partial^2\psi}{\partial y^2} = \left(\frac{180}{\pi}\right)^2 \frac{H_\eta^2\psi_{\xi\xi} + H_\xi^2\psi_{\eta\eta} - 2D\psi_{\xi\eta} + A\psi_\xi + B\psi_\eta}{J^2\cos^2\varphi}\,, \tag{12}$$

where

$$H_\xi^2 \equiv x_\xi^2 + y_\xi^2 \cos^2\varphi\,,\quad H_\eta^2 \equiv x_\eta^2 + y_\eta^2 \cos^2\varphi\,,\quad D \equiv x_\xi x_\eta + y_\xi y_\eta \cos^2\varphi\,, \tag{13}$$

$$A \equiv J\left[y_\eta \frac{\partial}{\partial\xi}\frac{y_\eta}{J} - y_\xi \frac{\partial}{\partial\eta}\frac{y_\eta}{J} - x_\xi \frac{\partial}{\partial\eta}\frac{x_\eta}{J} + x_\eta \frac{\partial}{\partial\xi}\frac{x_\eta}{J}\right] + J\cos\varphi \sin\varphi\, x_\eta\,, \tag{14}$$

$$B = J\left[-y_\eta \frac{\partial}{\partial\xi}\frac{y_\xi}{J} + y_\xi \frac{\partial}{\partial\eta}\frac{y_\xi}{J} + x_\xi \frac{\partial}{\partial\eta}\frac{x_\xi}{J} - x_\eta \frac{\partial}{\partial\xi}\frac{x_\xi}{J}\right] - J\cos\varphi \sin\varphi\, x_\xi\,, \tag{15}$$

4. The Difference Scheme for Mesh Generation

A number of different techniques for numerical generation of adaptive grids are presently available in the literature. It goes beyond the scope of present short note to discuss them here. We make use of the following elliptic grid generator

$$\frac{\partial}{\partial\xi} f\frac{\partial x}{\partial\xi} + \frac{\partial}{\partial\eta} f\frac{\partial x}{\partial\eta} = 0\,,\quad \frac{\partial}{\partial\xi} f\frac{\partial y}{\partial\xi} + \frac{\partial}{\partial\eta} f\frac{\partial y}{\partial\eta} = 0\,,\quad f \equiv f(x,y;t)\,. \tag{16}$$

where the function f(x,y,t) is at our disposal to govern the mesh. One is referred for details to [10], [11] and [12] where the related numerical technique is developed. It only suffices here to mention that in the regions where function f takes larger values, the Jacobian of the resulted mesh is smaller and vice versa. (see [10]). Using the elliptic generator provides the necessary smoothness of the mesh.

Consider the case when the rectangular region of Limited-Area Model of INM

$$x_1 = -60^\circ\,, x_2 = 28^\circ\,,\quad y_1 = 21^\circ\,, y_2 = 65^\circ\,. \tag{17}$$

is mapped unto the unit square. Then the b. c. defining the boundary lines are simply the following

$$x = x_1, x_2 \quad for \quad \xi = 0,1\,,\quad y = y_1, y_2 \quad for \quad \eta = 0,1\,. \tag{18}$$

These are coupled by the conditions stemming from the requirement that the coordinate lines must be orthogonal to the boundaries, namely

$$y_\xi = 0 \quad for \quad \xi = 0,1\,;\quad x_\eta = 0 \quad for \quad \eta = 0,1\,. \tag{19}$$

Following [10], [11], [12] we solve the above boundary value problem by means of introducing time derivatives into both equations and applying an implicit splitting-type scheme. For the function x it reads

$$\frac{\tilde{x}_{ij} - x_{ij}^n}{\tau} = \Lambda_{\xi\xi}\tilde{x}_{ij} + \Lambda_{\eta\eta}x_{ij}^n\,,\quad \frac{x_{ij}^{n+1} - \tilde{x}_{ij}}{\tau} = \Lambda_{\eta\eta}\left(x_{ij}^{n+1} - x_{ij}^n\right) \tag{20}$$

where the $\Lambda_{\xi\xi}$ and $\Lambda_{\eta\eta}$ stand for the difference approximations of the respective second-order differential operators in (16). When the mesh is fixed the particular iterational algorithm is not so important because the

solution is used only after the convergence is attained. Hence the main reason to use an absolutely stable implicit scheme is to have a margin of stability for the case when the mesh is evolving with time not imposing on the time increment additional (and more restrictive) limitations than the scheme for the vorticity equation does.

The system (16) is solved on a following staggered uniform mesh (see Fig.1) in the $O\xi\eta$ plane:

$$\xi_{i-\frac{1}{2}} = (i-1.5)h_1, \quad for \quad i=1,2,\ldots,M+1; \quad h_1 = 1/M . \tag{21}$$

$$\eta_{j-\frac{1}{2}} = (j-1.5)h_2, \quad for \quad j=1,2,\ldots,N+1; \quad h_2 = 1/N . \tag{22}$$

Here M and N are the total numbers of grid lines in ξ and η directions, respectively.

The standard symmetric three-point differences are used, namely

$$\Lambda_{\xi\xi}\varphi_{i+\frac{1}{2},j+\frac{1}{2}} = \frac{1}{h_1^2}\left[f_{i,j+\frac{1}{2}}\varphi_{i-\frac{1}{2},j+\frac{1}{2}} - \left(f_{i,j+\frac{1}{2}}+f_{i+1,j+\frac{1}{2}}\right)\varphi_{i+\frac{1}{2},j+\frac{1}{2}} + f_{i+1,j+\frac{1}{2}}\varphi_{i+\frac{3}{2},j+\frac{1}{2}}\right] \tag{23}$$

$$\Lambda_{\eta\eta}\varphi_{i+\frac{1}{2},j+\frac{1}{2}} = \frac{1}{h_1^2}\left[f_{i+\frac{1}{2},j}\varphi_{i+\frac{1}{2},j-\frac{1}{2}} - \left(f_{i+\frac{1}{2},j}+f_{i+\frac{1}{2},j+1}\right)\varphi_{i+\frac{1}{2},j+\frac{1}{2}} + f_{i+\frac{1}{2},j+1}\varphi_{i+\frac{1}{2},j+\frac{3}{2}}\right] \tag{24}$$

Thereby each of the half-time steps (20) is reduced to three-diagonal linear algebraic system which is solved by means of Gaussian elimination with pivoting.

5. Results. The Fixed Grid

As above mentioned, the first mode of application of the mesh generation procedure is to create a fixed mesh which is denser in certain subregion of the main domain. When the mesh does not evolve with time, the problem of mesh generation decouples from the dynamical problem. As far as the latter is concerned, the differencing can be used to construct a conserving difference scheme in general curvilinear coordinates. The only difference is that, unlike the case of cartesian coordinates, the quantities that are conserved here are more complicated integrals of vorticity or its square (the coefficient of time derivative in eq.(4) makes the difference).

Respectively, the mesh generation problem is solved only once at the beginning of the calculations. Then the time in (20) becomes an iterational parameter and iterations are conducted until convergence is reached according to the following criterion

The optimal value of time increment τ depends in general on the function f. Its numerical value is selected in each case on the basis of numerical

$$\max_{ij}\left[\frac{\|x_{ij}^{n+1}-x_{ij}^{n}\|}{\|x_{ij}^{n+1}\|},\frac{\|y_{ij}^{n+1}-y_{ij}^{n}\|}{\|y_{ij}^{n+1}\|}\right] < 10^{-7} \qquad (25)$$

experiments.

On the base of extensive set of numerical experiments, we select the governing function f(x,y) of the form

$$f(x,y;t) = 1+\gamma\left[1+\alpha\left(\frac{x-x_c}{x_2-x_1}\right)^2+\alpha\left(\frac{y-y_c}{y_2-y_1}\right)^2\right]^{-1} \qquad (26)$$

which gives a sufficiently smooth transition of the coordinates from large grid sells to smaller ones. It is clear that x_c and y_c are the coordinates of the centre and the parameter α defines approximately the radius of a circle inside which the values of the localized function f are considerable and hence the coordinates lines must be denser. The quantitative measure for the density of coordinate lines is provided by the parameter γ.

The respective result for the case of Spain (x_c=4°, y_c=40°, α=13°) is shown in Fig.2. In order to give an idea about the accuracy of the difference approximation we present in Fig.2 the solutions with two different grid sizes. The first one is obtained with M=21, N=11 and is presented with thicker lines. The second one (the thinner lines) is obtained with M=81, N=41. It is seen that the results are virtually indistinguishable which means that the approximation of the difference scheme converges towards the solution of the differential problem.

6. Results. The Moving Mesh

It has already been shown in the precedence, that when the mesh is allowed to evolve with time, then the coordinate transformation affects as well the convective terms in the momentum equation. The latter become now more complicated but we can still apply the Arakawa scheme to each one of the Jacobians that appear in the transformed equation. Unfortunately the scheme is not more strictly conserving, as far as the terms connected with the coordinate functions x and y are concerned. However, it goes beyond the scope of the present work to construct a strictly conserving scheme. It suffices here to use any kind of scheme in order to elucidate the problems connected with the mesh generation.

Now, one is to establish the rule of correspondence between the function f from (16) and certain functional of solution reflecting the desired criterion of condensation. There could be many different ways of how to establish the sought criterion. The guideline is that in order to minimize the truncation error of the scheme, one must set function f roughly proportional to that error. The problem is that the expression of the truncation error is a complicate one involving higher-order derivatives. For this reason it is more practical to tune the mesh to the gradients of the solution, i.e. to the first-order derivatives. Therefore we set the governing function proportional to the slope of the stream function
where the metric coefficients H_ξ, H_η, the Jacobian J and the orthogonality condition D are defined in the above. The algorithm is implemented in an explicit manner and the said quantities are taken from the previous time stage. This makes the coordinates "lagging" from the dynamics. Quantitat-

$$f(x,y;t) = 1+\gamma\sqrt{\psi_x^2+\psi_y^2} \equiv 1+\gamma\frac{\sqrt{H_\eta^2\psi_\xi^2+H_\xi^2\psi_\eta^2-2D\psi_\xi\psi_\eta}}{J\cos\varphi}\ , \qquad (27)$$

ively speaking, however, this is immaterial because the correspondence of the regions of dense coordinate lines to the regions of high gradients of the solution need not be absolute. Rather it is suggestive and a compromise should be stricken between the quantitative satisfaction of (28) and the desired smoothness of the resulted mesh.

Note that the gradient of stream function in (27) is with respect to the "old" (cartesian) coordinates. It could not be with respect to the "new" coordinates because the ideal situation is when the gradients (or which is the same - the 2D slope) of ψ with respect to the actual coordinates, are almost constant.

The numerical values of the scaled stream function are of order 600 and hence its slope is of the same order. The numerical experiments show that the best results are obtained when γ lies in the range between 0.01 and 0.1 For $\gamma<0.01$ the mesh is not significantly affected by the gradients of the sought function while for $\gamma>0.1$, it is not smooth enough.

In Fig.3 and Fig.4 are shown the results for the evolving mesh. Fig.3 refers to the forecast for the stream function after 24 ours, while Fig.4 presents the results after 72 hours have passed. On the topmost graphs are shown the respective streamlines (note that the numerical values of scaled according to convention of [14] and are not equal to the respective values of the geopotential). Downwards are presented the patterns of the coordinates calculated for γ = 0.02, 0.05, 0.1, respectively.

7. Conclusions

The results of the present work show that the application of fixed curvilinear coordinates is cost effective in the sense that the resolution over specific area is significantly improved on the cost of marginal increase of the spent computational time. In addition, adding the vertical coordinate at each node of the adapted curvilinear horizontal system allows a straightforward generalization to 3D. However, the experience with the cost efficiency of introduction of a moving mesh is not unequivocal for 2D barotropic models. The horizontal gradients of the large-scale stream-function patterns are not large enough in order to justify the expenditures of calculating at each time stage a new distribution of the curvilinear mesh. It is clear, however, that the last conclusion may drastically change if the oblique fronts in 3D are to be properly represented by the mesh.

The first author acknowledges sabbatical fellowship from the Spanish Ministry of Science and Education.

References

[1] Skamarock W.C., Adaptive grid methods for numerical weather prediction, In Proc. "Numerical Methods in Atmospheric Models", 9-13 September 1991, ECMWF, Reading, UK, vol.1, pp.161-190.

[2] Fulton S. R., Ciesielski P.E., Schubert W.H., Multigrid methods for elliptic problems: a review, Monthly Wea. Rev., vol. 114 (1986), pp. 943-959.

[3] Altas I., J. W. Stephenson, A two-dimensional adaptive mesh generation method, J. Comput. Phys., vol.94 (1991), 201-224.

[4] Thompson J.F., Z.U.A. Warsi, Boundary-fitted coordinate systems for numerical solution of partial differential equations - a review, J. Comp. Phys., vol. 47 (1982), pp. 1-108.

[5] Thompson J.F., Z.U.A. Warsi, C.W. Mastin, Numerical Grid Generation: Foundations and Applications, North Holland, 1985, 483p.

[6] Anderson D.A., Adaptive grid methods for partial differential equations, In: "Advances in Grid Generation", K.N. Ghia and U. Ghia, edts., New-York, 1983, pp.1-20.

[7] Hawken D.F., J.J. Gottlieb, J.S. Hansen, Review of some adaptive node movement techniques in finite-element and finite-difference solutions of partial differential equations, J. Comput. Phys., vol. 95 (1991), pp. 254-302.

[8] Dietachmayer G.S., K.K. Droegemeier, Application of continuous dynamic grid adaptation techniques to meteorological modelling. Pat I: Basic formulation and accuracy, Month. Wea. Rev., vol.120 (1992), 1675-1722.

[9] Adams J., R. Garcia, B. Cross, J. Hack, D. Haidvogel, V. Pizzo, Applications of Multigrid software in the atmospheric sciences, Month. Wea. Rev., vol. 120 (1992), pp.1447-1458.

[10] Christov C.I., Orthogonal Grids with Manageable Jacobians, In "Numerical Grid Generation", J. Thompson, Ed., Elsevier, 1982, pp. 897-904.

[11] Christov C.I., Canonical Adaptive Grids: Orthogonality versus Smoothness, Paper in preparation, 1992.

[12] Christov C.I., Numerical Generation of Adaptive Canonical Grids, To be presented on the 2nd USA Congress on Computational Mechanics, Washington, D.C., 16-18 August 1993.

[13] Haltiner G.J, Williams R.T., Numerical Prediction and Dynamic Meteorology, John Wiley $ Sons, New York, 1980, 477 p.

[14] Krishnamurthi T.N., Libro de ejercicios sobre Predicción Numérica del tiempo em los tropicos para la formacion del personal meteorologico de los clase I y II, OMM, nº669 (1989).

[15] Haseler J., Burridge D., Documentation for the ECMWF grid point model, Internal Report nº9, Research Dept. of ECMWF, 1977.

[16] Arakawa A, Computational Design for Long-Term Numerical Integrations of the Equations of Atmospheric motion, J. Comput. Physics, vol.1 (1966), 119-143.

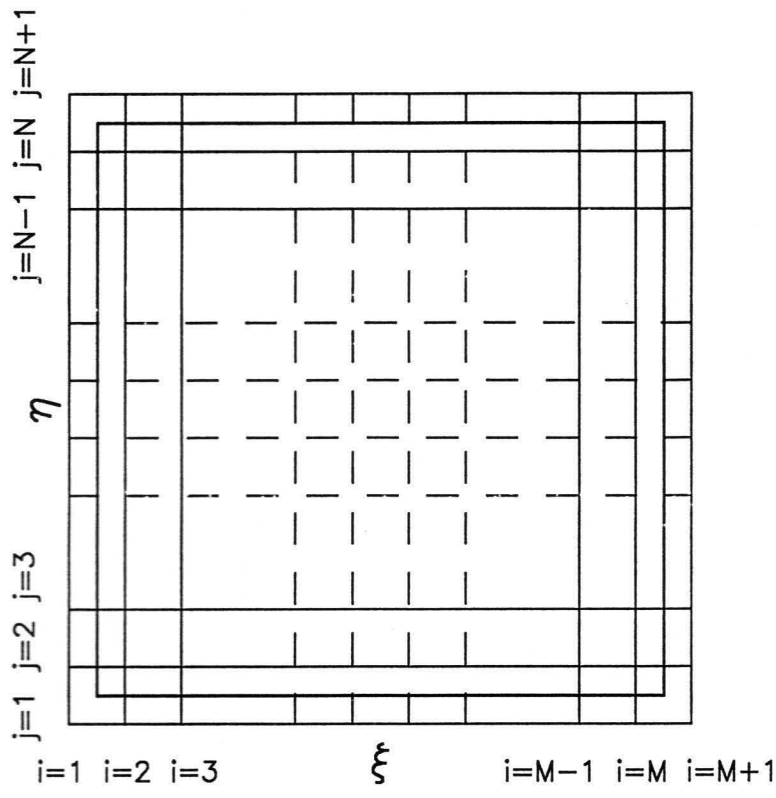
j=N+1
j=N
j=N−1
η
j=3
j=2
j=1
i=1
i=2
i=3
ξ
i=M−1
i=M
i=M+1

Fig. 1

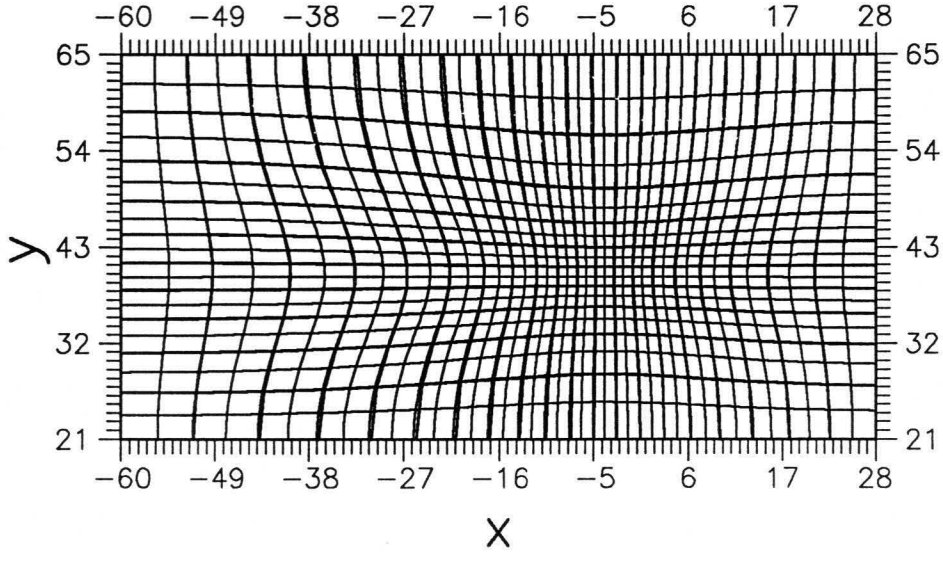
−60
−49
−38
−27
−16
−5
6
17
28
65
54
43
32
21
y
x

Fig. 2

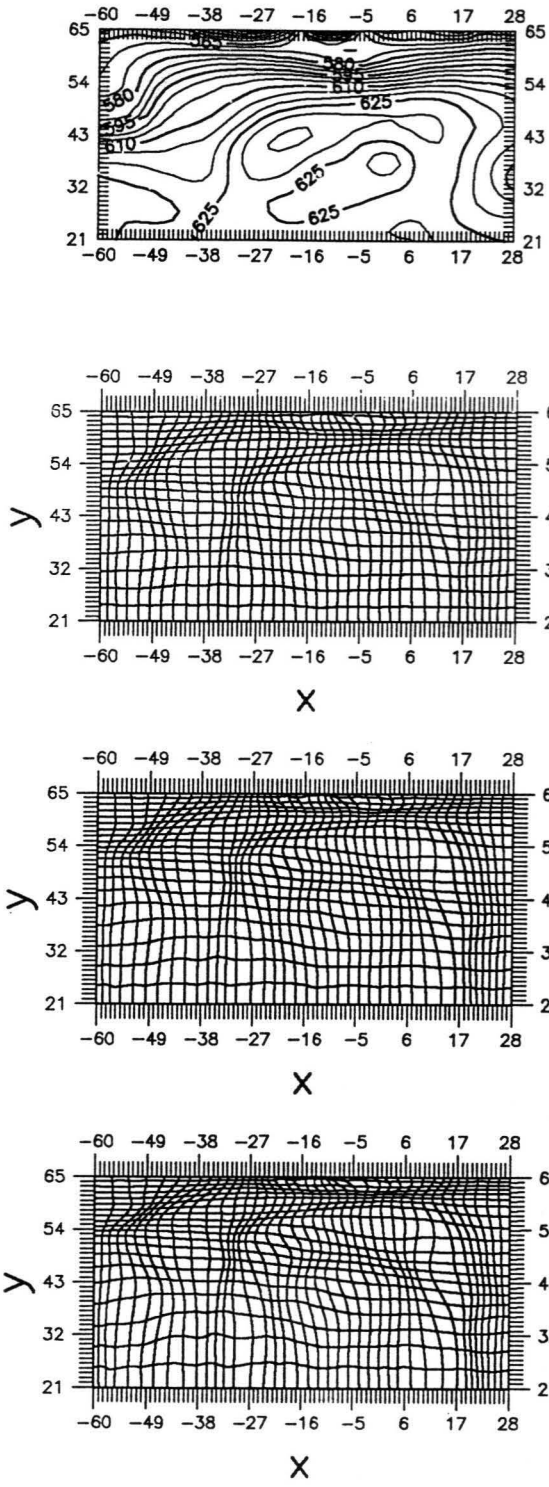
−60 −49 −38 −27 −16 −5 6 17 28
65 54 43 32 21
y
x
580
595
610
625

Fig. 3

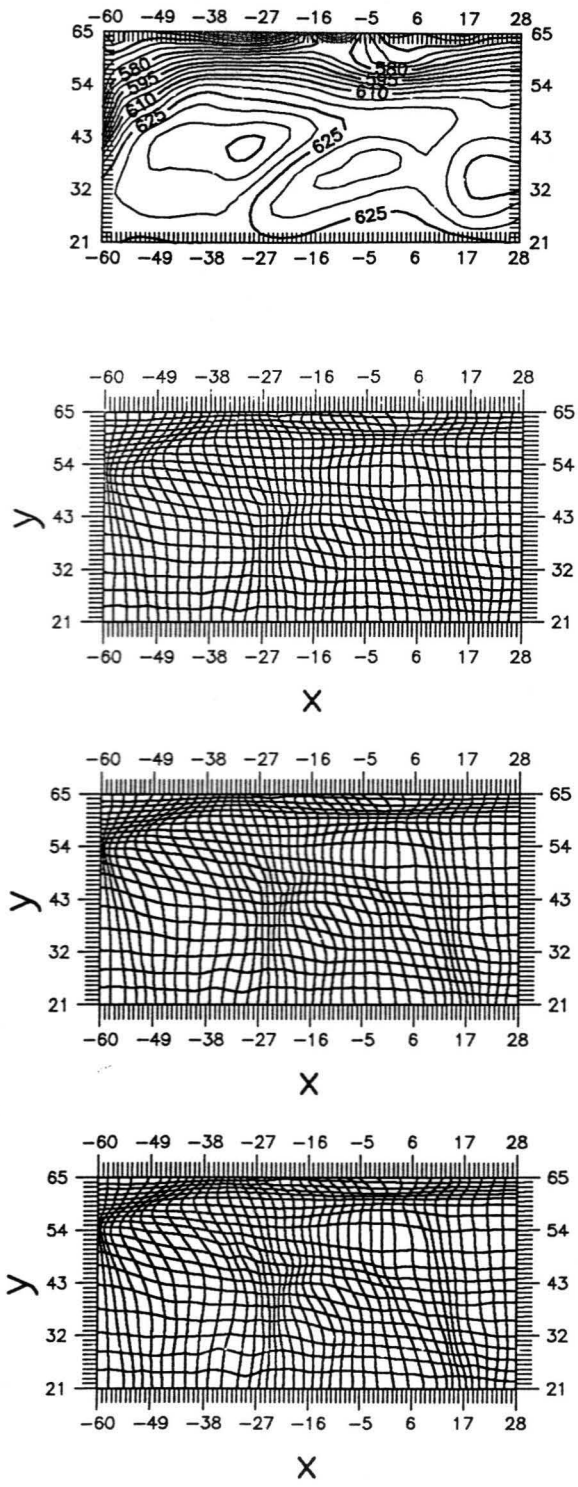
−60 −49 −38 −27 −16 −5 6 17 28
65 54 43 32 21
y
x
580
595
610
625

Fig. 4